



Research article

Effect of UV irradiation on the densification behavior, microstructure, and microwave dielectric properties of low temperature sintering Al₂O₃ ceramics

Hongxin Wu, W. Li *

School of Materials Science and Engineering, East China University of Science and Technology, Shanghai, 200237, China

ARTICLE INFO

Keywords:

Al₂O₃
UV irradiation
Low temperature sintering
Microwave dielectric properties

ABSTRACT

In this paper, Al₂O₃ ceramics co-doped with 0.3 wt%CuO–0.6 wt%TiO₂–0.1 wt%MnCO₃ (CTM, the same below) were prepared. The effect of CTM and UV irradiation on the sintering behavior, microstructure, and microwave dielectric properties have been investigated systematically. The results indicate that the sintering temperature of Al₂O₃ ceramics could be effectively decreased to about 1200 °C by adding 1 wt% CTM. UV irradiation can further increase the density of the Al₂O₃ ceramics, improve its microstructure and microwave dielectric properties. By using the Al₂O₃ powders UV irradiated for 15 min as raw materials, CTM co-doped Al₂O₃ ceramics can sintered at 1200 °C with a high density of 3.93 g/cm³ and a very high Q × f value of 175,086 GHz.

1. Introduction

With the arrival of the 5G era, microwave dielectric materials are receiving increasing attention. As a very important microwave dielectric material, Al₂O₃ ceramics are widely used in antennas, resonators, filters, and other equipment due to its high strength, corrosion resistance and outstanding microwave dielectric properties [1–3]. However, pure Al₂O₃ ceramics require a high temperature exceeding 1500 °C to be sintered [4], which does not meet the requirements of modern industrial green energy conservation. So, reducing the sintering temperature of Al₂O₃ ceramics is very important. The most effect way to reduce the sintering temperature is co-doping with different sintering aids such as TiO₂, CuO, MgO etc. [5,6]. For example, I-Wei Chen et al. [7] sintered Al₂O₃ ceramics with a high relative density of 99.3% at 1070 °C for 1 h by adding 0.9 mol% CuO + 0.9 mol% TiO₂+0.1 mol% B₂O₃+0.1 mol% MgO. Yang et al. [8] obtained Al₂O₃ ceramics with a high density of 3.92 g/cm³ at 975 °C by doping with 5 wt% 4CuO–TiO₂–2Nb₂O₅. Regretfully, its Q × f value is only 7400 GHz. Recently, we have conducted a series of studies on low-temperature sintering Al₂O₃ ceramics via different co-doping. By co-doping with 1.5 wt% CuO–3wt% Nb₂O₅–0.5 wt% ZrO₂, Al₂O₃ ceramics could be sintered at 1000 °C with a high density of 3.91 g/cm³ and a Q × f value of 15,541 GHz [9]. By co-doping with 0.3 wt% CuO–0.6 wt% TiO₂–0.05 wt% MgO, the Al₂O₃ could be sintered at 1150 °C with a high Q × f value of 109,616 GHz [10]. Another feasible way to decrease the sintering temperature is using powders with less agglomeration and high sintering activity. For example, Huang et al. [11] obtained Al₂O₃ ceramics with a high Q × f value of about 60,000 GHz at 1350 °C by using nano Al₂O₃ powder as raw materials.

In this paper, low temperature sintering Al₂O₃ ceramics have been prepared by co-doping with CTM, UV irradiation was applied to improve the dispersion and de-agglomeration of the raw Al₂O₃ powder for the first time. The effects and relevant mechanisms of CTM

* Corresponding author.

E-mail address: liweiwei@ecust.edu.cn (W. Li).

and UV irradiation on the density, microstructure, and dielectric properties of Al_2O_3 ceramics were investigated for the first time.

2. Experimental procedure

High-purity Al_2O_3 powder ($\alpha\text{-Al}_2\text{O}_3 > 99.95\%$) was used as the raw materials. First, the Al_2O_3 powder was divided into two equal parts. One part was used directly, another part was evenly spread in a watch glass and vertically illuminated with a UV lamp ($\lambda = 250 \pm 20$ nm, $P = 15$ W, Philips) for 15 min. Then both parts were mixed with CTM separately via a planetary ball mill at 90 rpm for 2 h. After drying, the powders were pressed into cylindrical samples with a diameter of 16 mm and a height of 8 mm. These pressed samples using Al_2O_3 powder with and without UV irradiation as raw materials were named as Sample-A and Sample-B respectively. Finally, both Sample-A and Sample-B were put into a muffle furnace and sintered at different temperatures (1150°C-1225 °C) for 4 h.

The specific surface area of the powder was examined by surface area and pore size analyzer (Quantachrome N42-26e). Specific surface area was calculated using Brunauer-Emmett-Teller (BET) method. The density of the samples was measured by the Archimedes drainage method. The phase composition of the samples was analyzed by using the Bruker D8 Advance X-ray diffractometer produced by Karlsruhe, Germany (Cu target $K\alpha$ rays, working voltage and current are 40 kV and 40 mA respectively, scanning step is 0.02, scanning range is $10^\circ\text{--}80^\circ$ (2θ), scanning speed is $6^\circ/\text{min}$). The Hakki-Coleman dielectric resonance network method and a network analyzer (E8362, Agilent Technologies, Loveland, CO) were used to measure the microwave dielectric properties. The TM-3030 field emission scanning electron microscope (accelerating voltage 15 kV) produced by Hitachi was used to observe the microstructure of the samples. Micro-area elemental analysis of the samples was carried out by a field Emission scanning electron microscope (FESEM, Gemini SEM 500, Germany) equipped with an energy dispersive spectrometer (EDS).

3. Results and discussion

Fig. 1 shows density curves of Sample-A and Sample-B. As shown in Fig. 1, the density of both the samples keeps increasing when the temperature rises from 1150 °C to 1200 °C. The highest density can be obtained at 1200 °C. Then, as the sintering temperature continues to rise, the densities begin to decrease. The highest density of 3.93 g/cm^3 can be obtained for Sample-A at 1200 °C.

There may be two reasons for the low-temperature densification behavior of both the samples. One is the forming of the liquid phase. Some investigations show that the eutectic formation temperature of $\text{CuO-CuO}_2\text{-Al}_2\text{O}_3$ is 1096 °C [12], the eutectic formation temperature of CuO-TiO_2 is 1000 °C [13], while the melting point of MnO_2 is only 535 °C. It can be reasonably inferred that several of Al_2O_3 , CuO , TiO_2 , and MnO_2 may form a liquid phase at relatively low temperatures, which can promoting the sintering process [10]. Another is the Cu^{2+} , Ti^{4+} , Mn^{4+} may diffuse into Al_2O_3 to form solid solution, distorting and activating the lattice, and further reduce the sintering temperature [14].

In Fig. 1, an interesting phenomenon can be found is that the density of Sample-A is always higher than that of Sample-B at the same temperature, which indicates that UV irradiation can effectively promote the sintering process. Although the real reason is unclear now, it may be related to the improvement of powder dispersion by UV irradiation. The specific surface area test results show that the BET values of the powder without UV irradiation is $2.16\text{ m}^2/\text{g}$ and $2.35\text{ m}^2/\text{g}$ before and after ball milling respectively, while for the powder with UV irradiation, these values increase to $2.63\text{ m}^2/\text{g}$ and $3.27\text{ m}^2/\text{g}$, which means that the Al_2O_3 powder could be de-agglomerated via UV radiation. Although the specific reasons need further investigation, we believe the de-agglomeration might be

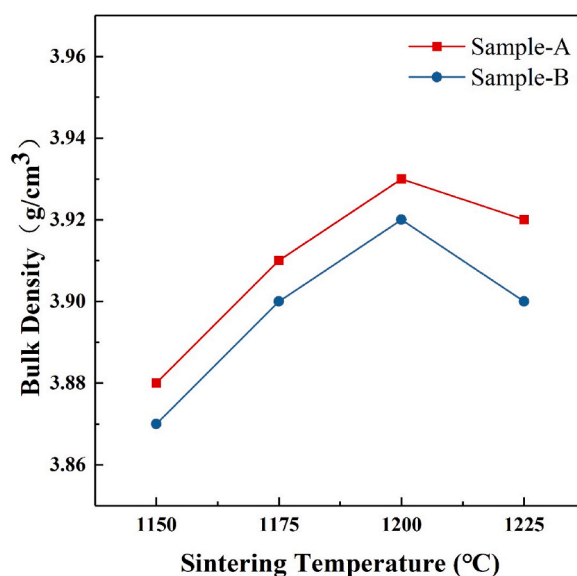


Fig. 1. Sintering density curve of Sample-A and Sample-B.

related to certain changes on the surface of the powder caused by UV irradiation, including better hydrophilicity and more oxygen vacancy as reported in our previous research [15].

Fig. 2 shows XRD diffraction patterns of the Sample-A and Sample-B. Only corundum phase (JCPDS file No.10-0173) can be detected in both the samples at different sintering temperatures, which means that if there is other phase present, either the content is very low or the phase is amorphous.

Fig. 3 is the SEM images of Sample-A and Sample-B. In Fig. 3, it can be seen that as the sintering temperature increases from 1150 °C to 1225 °C, the grain sizes in both Sample-A and Sample-B are continuously increasing. An interesting phenomenon is the grain distribution in Sample-A is much more uniform than that in Sample-B when the temperature ≥ 1175 °C. This phenomenon may be related to the improved dispersion performance of the powder after UV irradiation. As we know, agglomeration in the powder can easily grow into large grains due to the differential sintering [16,17], resulting in uneven grain size dispersion as shown in Sample-B. So, when the agglomerates are destroyed by UV irradiation, the grain distribution become much more uniform as shown in Sample-A.

Another phenomenon in Fig. 3 is the appearance of white matter on the surface of the samples. At 1150 °C, a very small amount of white spots can be observed in both samples. Then, as the temperature keep rising, the white dots increase obviously in Sample-B while their content keeps very limited in Sample-A. Combining the XRD spectrum analysis in Fig. 2, it can be reasonably inferred that these white spots are likely amorphous compounds. To further analyze these white spots, their composition was conducted by EDS testing and the results show that the white dots in Sample-A and Sample-B are 94.6%Al₂O₃-4.1%CuO-1.3%TiO₂ and 91.3%Al₂O₃-6.0%CuO-2.7%TiO₂ respectively. The content of CuO and TiO₂ in Sample-B is significantly higher while the content of Al₂O₃ is obviously lower. This difference could be explained by the different dispersibility of the raw Al₂O₃ powder. As mentioned earlier, the agglomeration of Al₂O₃ powder used in Sample-A is less, so the sintering additives dispersed in the Al₂O₃ powder more uniformly. Therefore, the white amorphous phase generated in Sample-A during the sintering process is finer, and the content of additives will be lower. Besides, there is no Mn present in the white dots, indicating that Mn is not involved in the low eutectic compounds, or their amount is extremely limited, which is lower than the detection limit of EDS.

Fig. 4 is the dielectric constant curves of Sample-A and Sample-B. As the sintering temperature increases, the dielectric constant of both Sample-A and Sample-B first increases and then decreases, maximum values can be reached at 1200 °C. At the same temperature, the dielectric constant of Sample-A is higher than that of Sample-B. Comparing Figs. 1 and 4, it can be found that the change trend of dielectric constant is consistent with the change trend of density. This phenomenon should be related to the lack of pores in higher density sintered bodies (the dielectric constant in the pores is approximately equal to 1).

Fig. 5 is the $Q \times f$ value of Sample-A and Sample-B. Similar to the dielectric constant, the $Q \times f$ values of Sample-A and Sample-B also first increase and then decrease with increasing temperature. However, there are significant differences between the two kinds of samples. When the temperature increased from 1150 °C to 1175 °C, the $Q \times f$ value of Sample-A is only slightly higher than that of Sample-B. Then as the temperature increased to 1200 °C, the $Q \times f$ value of Sample-B begin to decrease, while the $Q \times f$ value of Sample-A surprisingly increased to 175,086 GHz, which is 88% higher than the $Q \times f$ value of Sample-B. Finally, as the temperature rises to 1225 °C, the $Q \times f$ value of Sample-A begins to decrease, but it keeps much higher than that of Sample-B.

There are two possible reasons for the phenomenon in Fig. 5. One is the grain size and its uniformity. Many investigations show that larger grain size and higher uniformity are helpful to the increasing of $Q \times f$ value [17-21]. Another is the impure phase. Generally, the presence of impurities, especially amorphous impurities, can lead to a decrease of $Q \times f$ values [9,21,22]. As shown in Fig. 3, the grain

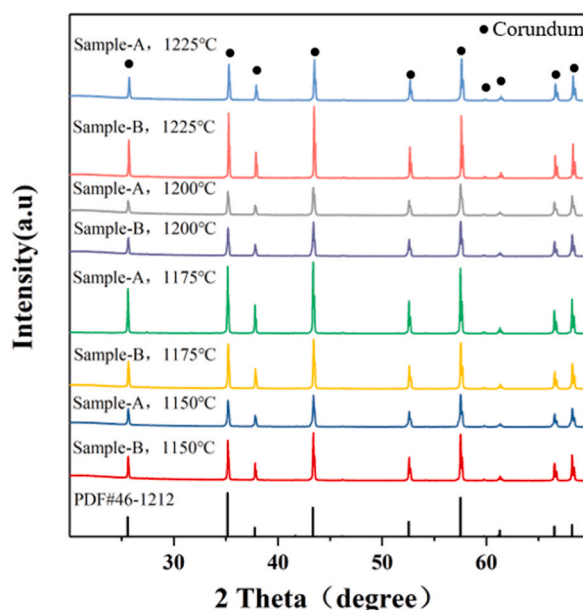


Fig. 2. XRD diffraction patterns of Sample-A and Sample-B.

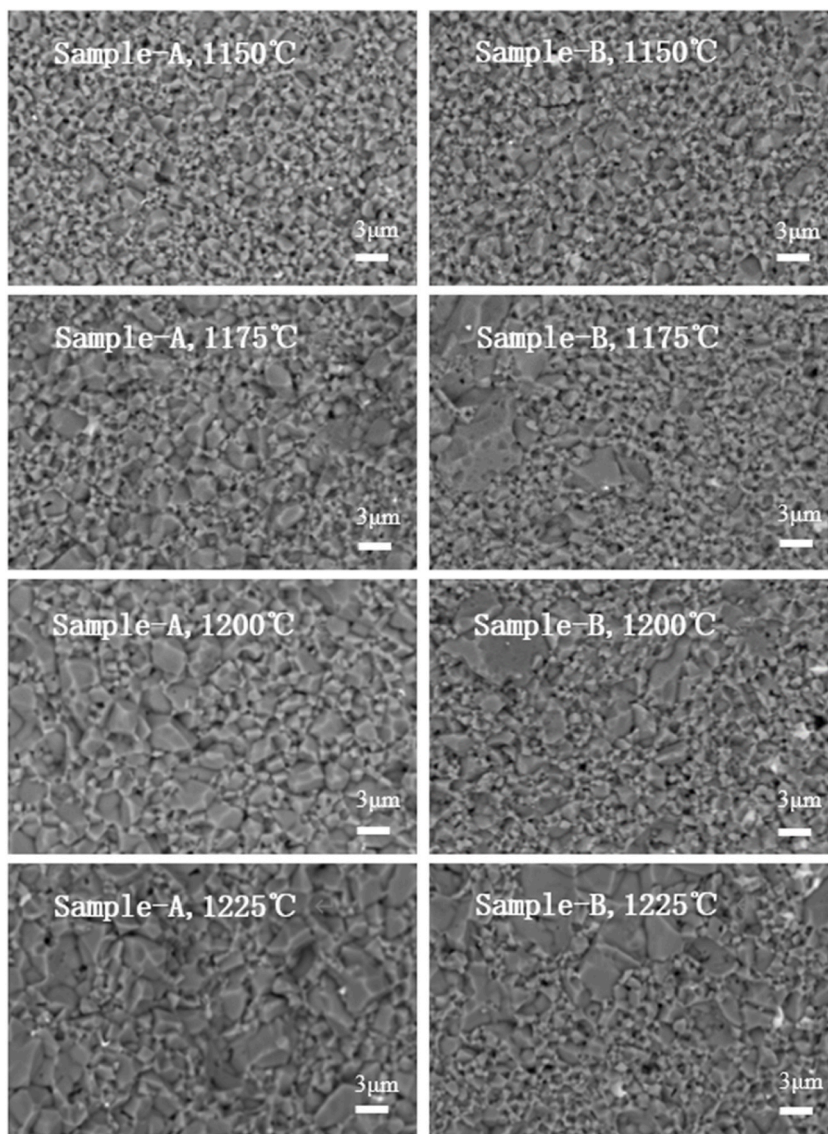


Fig. 3. SEM images of Sample-A and Sample-B.

size of both Sample-A and Sample-B increases obviously when the temperature rises from 1150 °C to 1175 °C, so the $Q \times f$ values increase. Due to the better uniformity of grain size, the $Q \times f$ value of Sample-A is higher. Then, as the sintering temperature rises to 1200 °C, the grains in Sample-A grow significantly, with most of the small grains disappeared and the uniformity becoming better. As a result, a much higher $Q \times f$ value could be obtained. On the contrary, although the grains in Sample-B continue to grow, they become more uneven and white amorphous spots begin to appear in large quantities, leading to a decrease of $Q \times f$ value. Finally, when the temperature rises to 1225 °C, as the white amorphous spots begin to increase, the $Q \times f$ value of Sample-A begins to decrease. Meanwhile, the $Q \times f$ value of Sample-B keeps to decrease as the white amorphous spots keep increasing.

4. Conclusions

- (1) The sintering temperature of Al_2O_3 ceramics can be effectively reduced via CTM co-doping. When 1 wt% CTM added, high relative densities ($\geq 97.24\%$) can be obtained at ≥ 1150 °C. The highest density can be reached at 1200 °C. The forming of the liquid phase and the solid solution might be the two reasons for the accelerating of the densification process.
- (2) UV irradiation can further improve the sintering behavior and the microstructure of Al_2O_3 ceramics. Higher densities can be obtained by using the UV irradiation treated Al_2O_3 powder as raw materials at the same sintering temperature. Meanwhile, the grain distribution becomes significantly more uniform. The reason for this phenomenon is attributed to the destructive effect of UV irradiation on the agglomeration in the Al_2O_3 powder.

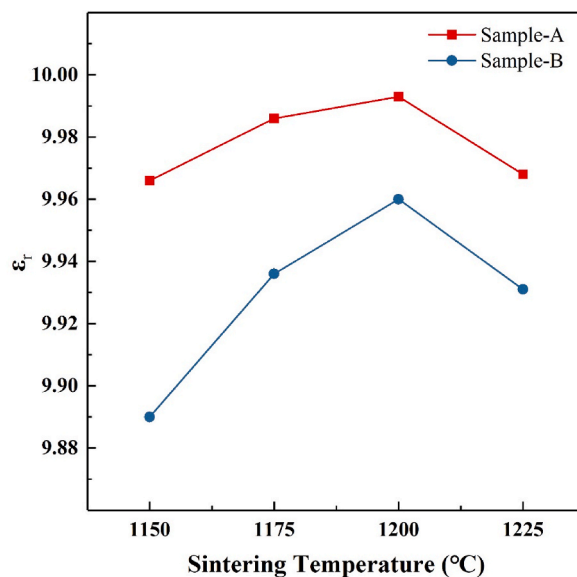


Fig. 4. Dielectric constant of Sample-A and Sample-B.

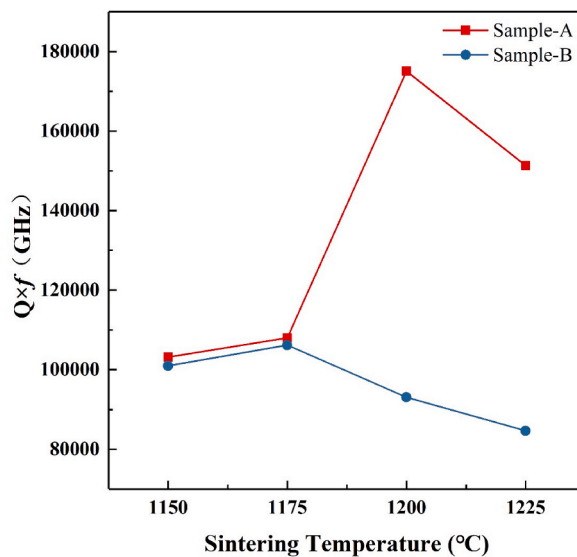


Fig. 5. $Q \times f$ value of Sample-A and Sample-B.

- (3) The CTM co-doped Al_2O_3 ceramics show fairly good dielectric properties, especially high $Q \times f$ values. When sintered at 1150–1175 °C, the $Q \times f$ value of all the samples is > 100000 GHz. UV irradiation can effectively improve the $Q \times f$ values. An astonishing high $Q \times f$ value of 175,086 GHz can be achieved after sintering at 1200 °C. The reason is that after UV irradiation treatment, the sintered sample has fewer grain boundaries, more uniform grain distribution, and fewer amorphous phases.

Data availability

The data that support the findings of this study are available from the corresponding author, [Li Wei], upon reasonable request.

CRediT authorship contribution statement

Hongxin Wu: Writing – original draft, Validation, Formal analysis, Data curation. **W. Li:** Writing – review & editing.

Declaration of competing interest

The authors declare that they have no known competing financial interests or personal relationships that could have appeared to influence the work reported in this paper.

References

- [1] H.S. Kim, M.Y. Seo, I.J. Kim, *Advanced engineering ceramics for semiconductor package technology*, in: 4th China International Conference on High-Performance Ceramics (CICC-4) Chengdu, PEOPLES R CHINA, 2005, pp. 1155–1158.
- [2] J.D. Breeze, X. Aupi, N.M. Alford, Ultralow loss polycrystalline alumina, *Appl. Phys. Lett.* 81 (2002) 5021–5023, <https://doi.org/10.1063/1.1532553>.
- [3] K.X. Song, S.Y. Wu, X.M. Chen, Effects of Y2O3 addition on microwave dielectric characteristics of Al2O3 ceramics, *Mater. Lett.* 61 (2007) 3357–3360, <https://doi.org/10.1016/j.matlet.2006.11.062>.
- [4] W.K. Seong, B.M. Ahn, Y.H. Min, G.T. Hwang, J.J. Choi, J.H. Choi, B.D. Hahn, Y.R. Cho, C.W. Ahn, Effect of Nb2O5 addition on microstructure and thermal/mechanical properties in zirconia-toughened alumina sintered at low temperature, *Ceram. Int.* 46 (2020) 23820–23827, <https://doi.org/10.1016/j.ceramint.2020.06.158>.
- [5] W.J. Si, R.M. Liu, The effect of doping on the dielectric loss of alumina ceramics, *Rare Met. Mater. Eng.* 36 (2007) 445–448, <https://doi.org/10.1002/pip.751>.
- [6] C. Chen, W. Li, Effect of Nb2O5 and MgO/Nb2O5 doping on densification, microstructure and wear resistance of alumina, *Ceram. Int.* 45 (2019) 18205–18209, <https://doi.org/10.1016/j.ceramint.2019.04.189>.
- [7] L.A. Xue, I.W. Chen, Low-temperature sintering of alumina with liquid-forming additives, *J. Am. Ceram. Soc.* 74 (1991) 2011–2013, <https://doi.org/10.1111/j.1151-2916.1991.tb07825.x>.
- [8] Y. Yang, M. Ma, F. Zhang, F. Liu, G. Chen, Z. Liu, Y. Li, Low-temperature sintering of Al2O3 ceramics doped with 4CuO-TiO2-2Nb2O5 composite oxide sintering aid, *J. Eur. Ceram. Soc.* 40 (2020) 5504–5510, <https://doi.org/10.1016/j.jeurceramsoc.2020.06.068>.
- [9] P. Zhang, H. Tao, W. Li, Low temperature sintering of Al2O3 microwave dielectric ceramics co-doped with 1.5wt%CuO-3wt%Nb2O5-0.5wt%ZrO2, *J. Mater. Sci. Mater. Electron.* 33 (2022) 15773–15778, <https://doi.org/10.1007/s10854-022-08479-0>.
- [10] G. Dong, W. Li, Microwave dielectric properties of Al2O3 ceramics sintered at low temperature, *Ceram. Int.* 47 (2021) 19955–19958, <https://doi.org/10.1016/j.ceramint.2021.03.330>.
- [11] C.L. Huang, J.J. Wang, C.Y. Huang, Sintering behavior and microwave dielectric properties of nano alpha-alumina, *Mater. Lett.* 59 (2005) 3746–3749, <https://doi.org/10.1016/j.matlet.2005.06.053>.
- [12] A.M.M. Gadalla, J. White, Equilibrium relationships in the system CuO-Cu2O-Al2O3, *Trans. Br. Ceram. Soc.* 63 (1964) 39–62, <https://www.scopus.com/inward/record.uri?eid=2-s2.0-0001890118&partnerID=40&md5=ba7afa95bf5328001597ae3b8dbb85f5>.
- [13] M.A. de la Rubia, J.J. Reinoso, P. Leret, J.J. Romero, J. de Frutos, J.F. Fernández, Experimental determination of the eutectic temperature in air of the CuO-TiO2 pseudobinary system, *J. Eur. Ceram. Soc.* 32 (2012) 71–76, <https://doi.org/10.1016/j.jeurceramsoc.2011.07.026>.
- [14] M. Sathiyakumar, F.D. Gnanam, Influence of additives on density, microstructure and mechanical properties of alumina, *J. Mater. Process. Technol.* 133 (2003) 282–286, [https://doi.org/10.1016/S0924-0136\(02\)00956-1](https://doi.org/10.1016/S0924-0136(02)00956-1).
- [15] Y. Song, W. Li, Effect of UV irradiation on powder dispersion, *Ceram. Int.* 46 (2020) 15695–15698, <https://doi.org/10.1016/j.ceramint.2020.02.238>.
- [16] J. Xu, R. Li, Q. Li, Effect of agglomeration on nucleation potency of inoculant particles in the Al-Nb-B master alloy: modeling and experiments, *Metall. Mater. Trans.* 52 (2021) 1077–1094, <https://doi.org/10.1007/s11661-020-06123-2>.
- [17] M.J. Keshvani, S. Katba, S. Jethva, M. Udeshi, D.D. Pandya, N.A. Shah, A. Ravalia, B. Kataria, D.G. Kuberkar, Grain Boundary Effects on the Structural, Microstructural and Transport Behavior of Sol-Gel Grown PrMnO3 Nanoparticles, 2017, <https://doi.org/10.1063/1.4982122>.
- [18] Q. Hu, J. Tang, Y. Teng, X. Zhao, T. Arslanov, R. Ahuja, Preparation and dielectric properties of La doped NBCCTO ceramics, *J. Electroceram.* 48 (2022) 117–126.
- [19] Z. Wang, H.N. Chen, W.W. Nian, J.H. Fan, Y.B. Li, X.Y. Wang, X.P. Ma, Grain boundary effect on dielectric properties of (Nd0.5Nb0.5)(x)Ti1-xO2 ceramics, *J. Alloys Compd.* 785 (2019) 875–882, <https://doi.org/10.1007/s10832-022-00280-z>.
- [20] D.S. Krueger, S.J. Lombardo, The effect of processing conditions and porosity on the electrical properties of Y2O3-doped SrTiO3 internal boundary layer capacitors, *J. Ceram. Process. Res.* 8 (2007) 31–37, <https://doi.org/10.1111/j.1744-7402.2007.02157.x>.
- [21] S.J. Penn, N.M. Alford, A. Templeton, X. Wang, M. Xu, M. Reece, K. Schrapel, Effect of porosity and grain size on the microwave dielectric properties of sintered alumina, *J. Am. Ceram. Soc.* 80 (2005) 1885–1888, <https://doi.org/10.1111/j.1151-2916.1997.tb03066.x>.
- [22] L. Liu, Y.W. Fang, X.F. Deng, W.D. Zhuang, B. Tang, S.R. Zhang, Crystal structures and microwave dielectric properties of (Ba1-xSrx)La4Ti4O15 (x=0.8-0.95) ceramics, *J. Inorg. Mater.* 27 (2012) 281–284, <https://doi.org/10.3724/sp.J.1077.2012.00281>.